

Screening of a charged particle by multivalent counterions in salty water: Strong charge inversion

T. T. Nguyen, A. Yu. Grosberg, and B. I. Shklovskii

Department of Physics, University of Minnesota, 116 Church St. Southeast, Minneapolis, Minnesota 55455

Screening of a macroion such as a charged solid particle, a charged membrane, double helix DNA or actin by multivalent counterions is considered. Small colloidal particles, charged micelles, short or long polyelectrolytes can play the role of multivalent counterions. Due to strong lateral repulsion at the surface of macroion such multivalent counterions form a strongly correlated liquid, with the short range order resembling that of a Wigner crystal. These correlations create additional binding of multivalent counterions to the macroion surface with binding energy larger than $k_B T$. As a result even for a moderate concentration of multivalent counterions in the solution, their total charge at the surface of macroion exceeds the bare macroion charge in absolute value. Therefore, the net charge of the macroion inverts its sign. In the presence of a high concentration of monovalent salt the absolute value of inverted charge can be larger than the bare one. This strong inversion of charge can be observed by electrophoresis or by direct counting of multivalent counterions.

PACS numbers: 87.14.Gg, 87.16.Dg, 87.15.Tt

I. INTRODUCTION

Charge inversion is a phenomenon in which a charged particle (a macroion) strongly binds so many counterions in a water solution that its net charge changes sign. As shown below the binding energy of a counterion with large charge Z is larger than $k_B T$, so that this net charge is easily observable; for instance, it is the net charge that determines linear transport properties, such as particle drift in a weak field electrophoresis. Charge inversion is possible for a variety of macroions, ranging from the charged surface of mica or other solids to charged lipid membranes, DNA or actin. Multivalent metallic ions, small colloidal particles, charged micelles, short or long polyelectrolytes can play the role of multivalent counterions. Recently, charge inversion has attracted significant attention¹⁻⁹.

Charge inversion is of special interest for the delivery of genes to the living cell for the purpose of the gene therapy. The problem is that both bare DNA and a cell surface are negatively charged and repel each other, so that DNA does not approach the cell surface. The goal is to screen DNA in such a way that the resulting complex is positive¹⁰. Multivalent counterions can be used for this purpose. The charge inversion depends on the surface charge density, so the cell surface charge can still be negative when DNA charge is inverted.

Charge inversion can be also thought of as an over-screening. Indeed, the simplest screening atmosphere, familiar from linear Debye-Hückel theory, compensates at any finite distance only a part of the macroion charge. It can be proven that this property holds also in non-linear Poisson-Boltzmann (PB) theory. The statement that the net charge preserves sign of the bare charge agrees with the common sense. One can think that this statement is even more universal than results of PB equation. It was shown¹⁻³, however, that this presumption of

common sense fails for screening by Z -valent counterions (Z -ions) with large Z , such as charged colloidal particles, micelles or rigid polyelectrolytes, because there are strong repulsive correlations between them when they are bound to the surface of a macroion. As a result, Z -ions form strongly correlated liquid with properties resembling a Wigner crystal (WC) at the macroion surface. The negative chemical potential of this liquid leads to an additional "correlation" attraction of Z -ions to the surface. This effect is beyond the mean field PB theory, and charge inversion is its most spectacular manifestation.

Let us demonstrate fundamental role of lateral correlations between Z -ions for a simple model. Imagine a hard-core sphere with radius b and with negative charge $-Q$ screened by two spherical positive Z -ions with radius a . One can see that if Coulomb repulsion between Z -ions is much larger than $k_B T$ they are situated on opposite sides of the negative sphere (Fig. 1a).

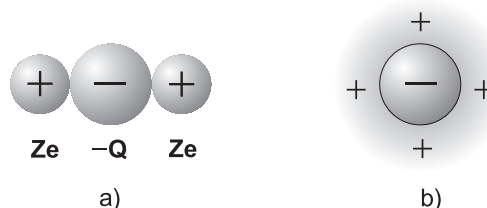


FIG. 1. a) A toy model of charge inversion. b) PB approximation does not lead to charge inversion.

If $Q > Ze/2$, each Z -ion is bound because the energy required to remove it to infinity $QZe/(a+b) - Z^2 e^2/2(a+b)$ is positive. Thus, the charge of the whole complex $Q^* = -Q + 2Ze$ can be positive. For example, $Q^* = 3Ze/2 = 3Q$ at $Q = Ze/2$. This example demonstrates the possibility of an almost 300% charge inversion. It is obviously a result of the correlation between Z -ions

which avoid each other and reside on opposite sides of the negative charge. On the other hand, the description of screening of the central sphere in the PB approximation smears the positive charge, as shown on Fig. 1b and does not lead to the charge inversion. Indeed, in this case charge accumulates in spherically symmetric screening atmosphere only until the point of neutrality at which electric field reverses its sign and attraction is replaced by repulsion.

Weak charge inversion can be also obtained as a trivial result of Z -ions discreteness without correlations. Indeed, discrete Z -ions can over-screen by a fraction of the "charge quantum" Ze . For example, if central charge $-Q = -Ze/2$ binds one Z -ion, the net charge of the complex is $Q^* = Ze/2$. This charge is, however, three times smaller than the charge $3Ze/2$ which we obtained above for screening of the same charge $-Ze/2$ by two correlated Z -ions, so that for the same Q and Z correlations lead to stronger charge inversion.

Difference between charge inversion, obtained with and without correlations becomes dramatic for a large sphere with a macroscopic charge $Q \gg Ze$. In this case, discreteness by itself can lead to inverted charge limited by Ze . On the other hand, it was predicted³ and confirmed by numerical simulations¹¹ that due to correlation between Z -ions which leads to their WC-like short range order on the surface of the sphere, the net inverted charge can reach

$$Q^* = 0.84\sqrt{QZe}, \quad (1)$$

i. e. can be much larger than the charge quantum Ze . This charge is still smaller than Q because of limitations imposed by the very large charging energy of the macroscopic net charge.

In this paper, we consider systems in which inverted charge can be even larger than what Eq. (1) predicts. Specifically, we consider the problem of screening by Z -ions in the presence of monovalent salt, such as NaCl, in solution. This is a more practical situation than the salt-free one considered in Ref. 2,3. Monovalent salt screens long range Coulomb interactions stronger than short range lateral correlations between adsorbed Z -ions. Therefore, screening diminishes the charging energy of the macroion much stronger than the correlation energy of Z -ions. As a result, the inverted charge Q^* becomes larger than that predicted by Eq. (1) and scales *linearly* with Q . The amount of charge inversion at strong screening is limited only by the fact that the binding energy of Z -ions becomes eventually lower than $k_B T$, in which case it is no longer meaningful to speak about binding or adsorption. Nevertheless, remaining within the strong binding regime, we demonstrate on many examples throughout this work, that the inverted charge, in terms of its absolute value, can be larger than the original bare charge, sometimes even by a factor up to 3. We call this phenomenon *strong* or *giant charge inversion* and its prediction and theory are the main results of our paper

(A brief preliminary version of this paper is given in Ref. 12).

Since, in the presence of a sufficient concentration of salt, the macroion is screened at the distance smaller than its size, the macroion can be thought of as an over-screened surface, with inverted charge Q^* proportional to the surface area. In this sense, overall shape of the macroion and its surface is irrelevant, at least to a first approximation. Therefore, we consider screening of a planar macroion surface with a negative surface charge density $-\sigma$ by finite concentration, N , of positive Z -ions, and concentration ZN of neutralizing monovalent coions, and a large concentration N_1 of a monovalent salt. Correspondingly, we assume that all interactions are screened with Debye-Hückel screening length $r_s = (8\pi l_B N_1)^{-1/2}$, where $l_B = e^2/(Dk_B T)$ is the Bjerrum length, e is the charge of a proton, $D \simeq 80$ is the dielectric constant of water. At small enough r_s , the method of a new boundary condition for the PB equation suggested in Ref. 2,3 becomes less convenient and in this paper we develop more universal and direct theoretical approach to charge inversion problem.

Our goal is to calculate the two-dimensional concentration n of Z -ions at the plane as a function of r_s and N . In other words, we want to find the net charge density of the plane

$$\sigma^* = -\sigma + Zen. \quad (2)$$

In particular, we are interested in the maximal value of the "inversion ratio", σ^*/σ , which can be reached at large enough N . The subtle physical meaning of σ^* should be clearly explained. Indeed, the entire system, macroion plus overcharging Z -ions, is, of course, neutralized by the monovalent ions. One can ask then, what is the meaning of charge inversion? In other words, what is the justification of definition of Eq. (2) which disregards monovalent ions?

To answer we note that under realistic conditions, every Z -ion, when on the macroion surface, is attached to the macroion with energy well in excess of $k_B T$. At the same time, monovalent ions, maintaining electroneutrality over the distances of order r_s , interact with the macroion with energies less than $k_B T$ each. It is this very distinction that led us to define the net charge of the macroion including adsorbed Z -ions and excluding monovalent ions (2). Our definition is physically justified, because, as we shall show now, it has direct experimental relevance. Indeed, let us imagine an electrophoresis experiment in which all ions are subjected to a weak external electric field such that the current is linear in the applied field. Sufficiently weak external field does not affect the strong (above $k_B T$) attachment of Z -ions to the macroion. In other words, the macroion coated with bound Z -ions drifts in the field as a single body. On the other hand, the surrounding atmosphere of monovalent ions, smeared over the distances about r_s , drifts with respect to the macroion. Presenting linear electrophoretic

mobility of a macroion as a ratio of effective charge to effective friction, we conclude that only Z -ions contribute to the former, while monovalent ions contribute only to the latter. In particular, and most importantly, the *sign* of the effect - in which direction the macroion moves, along the field or against the field - is determined by the sign of the net charge σ^* which, once again, includes Z -ions and does not include monovalent ones. Furthermore, for a macroion with simple (e.g. spherical) shape, the absolute value of the net macroion charge can be also found using the mobility measurements and the standard theory of friction in electrolytes¹³.

Similar logic suggests the principal possibility to count adsorbed Z -ions using atomic force microscope. Indeed, strongly adsorbed Z -ions can conceivably withstand a weak perturbation caused by the apparatus, while the neutralizing atmosphere of monovalent ions cannot. In this case, flipped sign of σ^* means "overpopulation": there are more bound Z -ions than neutrality condition implies.

Now, as we have formulated major goal of the paper, let us describe briefly its structure and main results. In Sec. II - IV we consider screening of a charged surface by compact Z -ions such as charged colloidal particles, micelles or short polyelectrolytes, which can be modeled as a sphere with radius a . We call such Z -ions "spherical". Spherical ions form correlated liquid with properties similar to two-dimensional WC (Fig. 2).

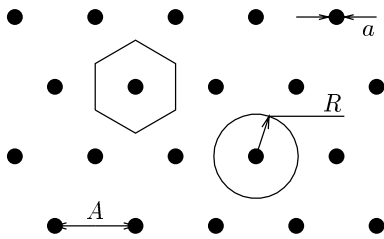


FIG. 2. Wigner crystal of Z -ions on the background of surface charge. A hexagonal Wigner-Seitz cell and its simplified version as a disk with radius R are shown.

In Sec. II we begin with screening of the simplest macroion which is a thin charged sheet immersed in water solution (Fig. 3a). This lets us to postpone the complication related to image potential which appears for a more realistic macroion which is a thick insulator charged at the surface (Fig. 3b). We calculate analytically the dependence of the inversion ratio, σ^*/σ , on r_s in two limiting cases $r_s \gg R_0$ and $r_s \ll R_0$, where $R_0 = (\pi\sigma/Ze)^{-1/2}$ is the radius of a Wigner-Seitz cell at the neutral point $n = \sigma/Ze$ (we approximate the hexagon by a disk). We find that at $r_s \gg R_0$

$$\sigma^*/\sigma = 0.83(R_0/r_s) = 0.83\zeta^{1/2}, \quad (\zeta \ll 1) \quad (3)$$

where $\zeta = Ze/\pi\sigma r_s^2 = (R_0/r_s)^2$. At $r_s \ll R_0$

$$\frac{\sigma^*}{\sigma} = \frac{2\pi\zeta}{\sqrt{3} \ln^2 \zeta}, \quad (\zeta \gg 1). \quad (4)$$

Thus σ^*/σ grows with decreasing r_s and can become larger than 100%. We also present numerical calculation of the full dependence of the inversion ratio on ζ .

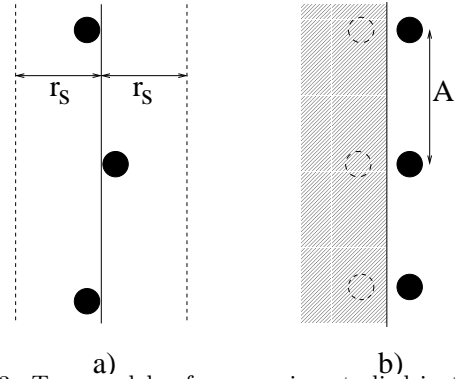


FIG. 3. Two models of a macroion studied in this paper. Z -ions are shown by full circles. a) Thin charged plane immersed in water. The dashed lines show the position of effective capacitor plates related to the screening charges. b) The surface of a large macroion. Image charges are shown by broken circles.

In Sec. III we discuss effects related to finite size of Z -ion. It is well known¹⁴ that monovalent ions can condense on the surface of a small and strongly charged spherical Z -ion. As a result, instead of the bare charge of Z -ions in Eqs. (3) and (4) one should use the net charge of Z -ions, which is substantially smaller. Thus, condensation puts a limit for the inversion ratio. The net charge grows with the radius a of the Z -ion. Therefore, we study in this section the case when $r_s \ll a \ll R_0$ and showed that the largest inversion ratio for spherical ions can reach a few hundred percent.

Sec. IV is devoted to more realistic macroions which have a thick insulating body with dielectric constant much smaller than that of water. In this case each Z -ion has an image charge of the same sign and magnitude. Image charge repels Z -ion and pushes WC away from the surface. In this case charge inversion is studied numerically in all the range of r_s or ζ . The result turns out to be remarkably simple: at $\zeta < 100$, the inversion ratio is twice smaller than for the case of the charged sheet immersed in water. A simple interpretation of this result will be given in Sec. IV.

In Sec. V and VI we study adsorption of long rod-like Z -ions with negative linear charge bare density $-\eta_0$ on a surface with a positive charge density σ . (We changed the signs of both surface and Z -ion charges to be closer to the practical case when DNA double helices are adsorbed on a positive surface.) Due to the strong lateral repulsion, charged rods tend to be parallel to each other and have a short range order of an one-dimensional WC (Fig. 4). In the Ref. 15 one can find beautiful atomic force microscopy pictures of almost perfect one-dimensional WC of DNA double helices on a positive membrane. The

adsorption of another rigid polyelectrolyte, PDDA, was studied in Ref. 16. Here we concentrate on the case of DNA.

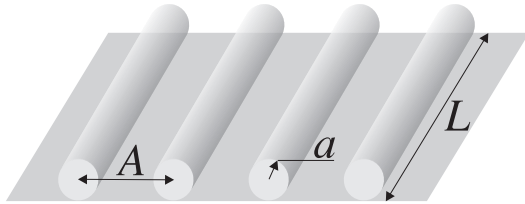


FIG. 4. Rod-like negative Z -ions such as double helix DNA are adsorbed on a positive uniformly charged plane. Strong Coulomb repulsion of rods leads to one-dimensional crystallization with lattice constant A .

It is well known that for DNA, the bare charge density, $-\eta_0$ is four times larger than the critical density $-\eta_c = -Dk_B T/e$ of the Onsager-Manning condensation¹⁷. According to the solution of nonlinear PB equation, most of the bare charge of an isolated DNA is compensated by positive monovalent ions residing at its surface so that the net charge of DNA is equal to $-\eta_c$. The net charge of DNA adsorbed on a charged surface may differ from $-\eta_c$ due to the repulsion of positive monovalent ions condensed on DNA from the charged surface. We, however, show that in the case of strong screening, $r_s \ll A_0$ ($A_0 = \eta_c/\sigma$), the potential of the surface is so weak that the net charge, $-\eta$, of each adsorbed DNA is still equal to $-\eta_c$. Simultaneously, at $r_s \ll A_0$ the Debye-Hückel approximation can be used to describe screening of the charged surface by monovalent salt. In Sec. V, these simplifications are used to study the case of strong screening. We show that the competition between the attraction of DNA to the surface and the repulsion of the neighbouring DNAs results in the negative net surface charge density $-\sigma^*$ and the charge inversion ratio, similar to Eq. (4):

$$\frac{\sigma^*}{\sigma} = \frac{\eta_c/\sigma r_s}{\ln(\eta_c/\sigma r_s)}, \quad (\eta_c/\sigma r_s \gg 1) \quad (5)$$

Thus the inversion ratio grows with decreasing r_s as in the spherical Z -ion case. At small enough r_s and σ , the inversion ratio can reach 400%. This is larger than for spherical ions because in this case, due to the large persistence length of DNA, the correlation energy remains large and WC-like short range order is preserved at smaller σr_s . An expression similar Eq. (5) has been recently derived for the case of polyelectrolyte with small absolute value of the linear charge density, $\eta_0 \ll \eta_c$, and strong screening ($r_s \ll A$) when screening of both the charged surface and the polyelectrolyte can be treated in Debye-Hückel approximation⁶. The result of Ref. 6 can be obtained if we replace the net charge η_c by the bare charge η_0 in Eq. (5).

In Sec. VI we study the adsorption of DNA rods in the case of weak screening by monovalent salt, $r_s \gg A_0$.

In this case, screening of the overcharged plane by monovalent salt becomes strongly nonlinear, with the Gouy-Chapman screening length $\lambda = e/(\pi l_B \sigma^*)$ much smaller than r_s . Simultaneously, the charge of macroion repels monovalent ions so that some of them are released from DNA. As a result the absolute value of the net linear charge density of a rod, η , is larger than η_c . We derived two nonlinear equations for unknown σ^* and η . Their solution at $r_s \gg A_0$ gives:

$$\frac{\sigma^*}{\sigma} = \frac{\eta_c}{\pi a \sigma} \exp\left(-\sqrt{\ln \frac{r_s}{a} \ln \frac{A_0}{2\pi a}}\right), \quad (6)$$

$$\eta = \eta_c \sqrt{\frac{\ln(r_s/a)}{\ln(A_0/2\pi a)}}. \quad (7)$$

At $r_s \simeq A_0$ we get $\eta \simeq \eta_c$, $\lambda \simeq r_s$ and $\sigma^*/\sigma \simeq 1$ so that Eq. (6) matches the strong screening result of Eq. (5). Since η can not be smaller than η_c , the fact that $\eta \simeq \eta_c$ already at $r_s \simeq A_0$ proves that at $r_s \ll A_0$, indeed, $\eta \simeq \eta_c$.

In Sec. VII we return to spherical Z -ions and derive the system of nonlinear equations which is similar to one derived in Sec. VI for rod-like ones. This system lets us justify the use of Debye-Hückel approximation for screening of overcharged surface (Sec. II) at r_s smaller than r_m , where $r_m = a \exp(R_0/1.65a)$ is an exponentially large length. We show that even at $r_s \gg r_m$ nonlinear equations lead only to a small correction to the power of r_s in Eq. (3).

In Sec. I-VII we assume that the surface charges of a macroion are frozen and can not move. In Sec. VIII we explore the role of the mobility of these charges. Surface charge can be mobile, for example, on charged liquid membrane where hydrophilic heads can move along the surface. If a membrane surface has heads with two different charges, for example, 0 and $-e$, the negative ones can replace the neutral ones near the positive Z -ion, thus accumulating around it and binding it stronger to the surface. We show that this effect enhances charge inversion substantially. We conclude in Sec. IX.

II. SCREENING OF CHARGED SHEET BY SPHERICAL Z -IONS

Assume that a plane with the charge density $-\sigma$ is immersed in water (Fig. 3a) and is covered by Z -ions with two-dimensional concentration n . Integrating out all the monovalent ion degrees of freedom, or, equivalently, considering all interactions screened at the distance r_s , we can write down the free energy per unit area in the form

$$\mathcal{F} = \pi \sigma^2 r_s / D - 2\pi \sigma r_s Z e n / D + F_{ZZ} + F_{id}, \quad (8)$$

where the four terms are responsible, respectively, for the self interaction of the charged plane, for the interaction

between Z -ions and the plane, for pair interactions between Z -ions and for the entropy of ideal two-dimensional gas of Z -ions. Using Eq. (2) one can rewrite Eq. (8) as

$$\mathcal{F} = \pi(\sigma^*)^2 r_s / D + F_{OCP}, \quad (9)$$

where $F_{OCP} = F_c + F_{id}$ is the free energy of the same system of Z -ions residing on a neutralizing background with surface charge density $-Zen$, which is conventionally referred to as one component plasma (OCP), and

$$F_c = -\pi(Zen)^2 r_s / D + F_{ZZ} \quad (10)$$

is the correlation part of F_{OCP} . The transformation from Eq. (8) to Eq. (9) can be simply interpreted as the addition of uniform charge densities $-\sigma^*$ and σ^* to the plane. The first addition makes a neutral OCP on the plane. The second addition creates two planar capacitors with negative charges on both sides of the plane which screen the inverted charge of the plane at the distance r_s (Fig. 3a). The first term of Eq. (9) is nothing but the energy of these two capacitors. There is no cross term corresponding to the interactions between the OCP and the capacitors because each planar capacitor creates a constant potential, $\psi(0) = 2\pi\sigma^*r_s/D$, at the neutral OCP.

Using Eq. (10), the electrochemical potential of Z -ions at the plane can be written as $\mu = Ze\psi(0) + \mu_{id} + \mu_c$, where μ_{id} and $\mu_c = \partial F_c / \partial n$ are the ideal and the correlation parts of the chemical potential of OCP. In equilibrium, μ is equal to the chemical potential, μ_b , of the ideal bulk solution, because in the bulk electrostatic potential $\psi = 0$. Using Eq. (9), we have:

$$2\pi\sigma^*r_s Ze/D = -\mu_c + (\mu_b - \mu_{id}). \quad (11)$$

As we show below, in most practical cases the correlation effect is rather strong, so that μ_c is negative and $|\mu_c| \gg k_B T$. Furthermore, strong correlations imply that short range order of Z -ions on the surface should be similar to that of triangular Wigner crystal (WC) since it delivers the lowest energy to OCP. Thus one can substitute the chemical potential of Wigner crystal, μ_{WC} , for μ_c . One can also write the difference of ideal parts of the bulk and the surface chemical potentials of Z -ions as

$$\mu_b - \mu_{id} = k_B T \ln(N_s/N), \quad (12)$$

where $N_s \sim n/a$ is the bulk concentration of Z -ions at the plane. Then Eq. (11) can be rewritten as

$$2\pi\sigma^*r_s Ze/D = k_B T \ln(N/N_0), \quad (13)$$

where $N_0 = N_s \exp(-|\mu_{WC}|/k_B T)$ is the concentration of Z -ions in the solution next to the charged plane, which plays the role of boundary condition for $N(x)$ when $x \rightarrow 0^{2,3}$. It is clear that when $N > N_0$, the net charge density σ^* is positive, i.e. has the sign opposite to the bare charge density $-\sigma$. The concentration N_0 is very small because $|\mu_{WC}|/k_B T \gg 1$. Therefore, it is easy to

achieve charge inversion. According to Eq. (12) at large enough N one can neglect second term of the right side of Eq. (11). This gives for the maximal inverted charge density

$$\sigma^* = \frac{D}{2\pi r_s} \frac{|\mu_{WC}|}{Ze}. \quad (14)$$

Eq. (14) has a very simple meaning: $|\mu_{WC}|/Ze$ is the "correlation" voltage which charges two above mentioned parallel capacitors with "distance between plates" r_s and total capacitance per unit area $D/(2\pi r_s)$.

To calculate the correlation voltage $|\mu_{WC}|/Ze$, we start from the case of weak screening when r_s is larger than the average distance between Z -ions. In this case, screening does not affect thermodynamic properties of WC. The energy per Z -ion $\varepsilon(n)$ of such Coulomb WC at $T = 0$ can be estimated as the energy of a Wigner-Seitz cell, because quadrupole-quadrupole interaction between neighbouring neutral Wigner-Seitz cells is very small. This gives

$$\varepsilon(n) = -(2 - 8/3\pi)Z^2 e^2 / RD \simeq -1.15Z^2 e^2 / RD, \quad (15)$$

where $R = (\pi n)^{-1/2}$ is the radius of a Wigner-Seitz cell. A more accurate calculation¹⁸ gives slightly higher energy:

$$\varepsilon(n) \simeq -1.11Z^2 e^2 / RD = -1.96n^{1/2}Z^2 e^2 / D. \quad (16)$$

One can discuss the role of a finite temperature on WC in terms of the inverse dimensionless temperature $\Gamma = Z^2 e^2 / (RDk_B T)$. We are interested in the case of large Γ . For example, at a typical $Zen = \sigma = 1.0 e/\text{nm}^2$ and at room temperature, $\Gamma = 10$ for $Z = 4$. Wigner crystal melts¹⁹ at $\Gamma = 130$, so that for $\Gamma < 130$ we deal with a strongly correlated liquid. Numerical calculations, however, confirm that at $\Gamma \gg 1$ thermodynamic properties of strongly correlated liquid are close to that of WC²⁰. Therefore, for an estimate of μ_c we can still write $F_c = n\varepsilon(n)$ and use

$$\mu_{WC} = \frac{\partial [n\varepsilon(n)]}{\partial n} = -1.65\Gamma k_B T = -1.65 \frac{Z^2 e^2}{RD}. \quad (17)$$

We see now that μ_{WC} is negative and $|\mu_{WC}| \gg k_B T$, so that Eq. (14) is justified. Substituting Eq. (17) into Eq. (14), we get $\sigma^* = 0.83Ze/(\pi r_s R)$. At $r_s \gg R$, charge density $\sigma^* \ll \sigma$, and $Zen \simeq \sigma$, one can replace R by $R_0 = (\sigma\pi/Ze)^{-1/2}$. This gives

$$\sigma^*/\sigma = 0.83\zeta^{1/2}, \quad (\zeta \ll 1), \quad (18)$$

where $\zeta = Ze/\pi\sigma r_s^2$ is the dimensionless charge of a Z -ion. Thus, at $r_s \gg R$ or $\zeta \ll 1$, inverted charge density grows with decreasing r_s . Extrapolating to $r_s = 2R_0$ where screening starts to modify the interaction between Z -ions substantially, we obtain $\sigma^* = 0.4\sigma$.

Now we switch to the case of strong screening, $r_s \ll R$, or $\zeta \gg 1$. It seems that in this case σ^* should decrease

with decreasing r_s , because screening reduces the energy of WC and leads to its melting. In fact, this is what eventually happens. However, there is a range of $r_s \ll R$ where the energy of WC is still large. In this range, as r_s decreases, the repulsion between Z -ions becomes weaker, what in turn makes it easier to pack more of them on the plane. Therefore, σ^* continues to grow with decreasing r_s .

Although we can continue to use the capacitor model to deal with the problem, this model loses its physical transparency when $r_s \ll R$, because there is no obvious spatial separation between the inverted charge σ^* and its screening atmosphere. Therefore, at $r_s \ll R$, we deal directly with the original free energy (8). The requirement that the chemical potential of Z -ion in the bulk solution equals that of Z -ions at the surface now reads

$$\frac{\partial F}{\partial n} = \mu_{id} - \mu_b, \quad (19)$$

where

$$F = -\frac{2\pi\sigma r_s Z e n}{D} + F_{ZZ} \quad (20)$$

is the interaction part of the total free energy (8) apart from the constant self-energy term $\pi\sigma^2 r_s/D$. According to Eq. (12), at large N when

$$\mu_b - \mu_{id} = k_B T \ln(N_s/N) \ll 2\pi\sigma r_s Z e/D, \quad (21)$$

we can neglect the difference in the ideal part of the free energy of Z -ion at the surface and in the bulk. Therefore, the condition of equilibrium (19) can be reduced to the problem of minimization of the free energy (20) with respect to n . This direct minimization has a very simple meaning: new Z -ions are attracted to the surface, but n saturates when the increase in the repulsion energy between Z -ions compensates this gain. Since this minimization balances the attraction to the surface with the repulsion between Z -ions, the inequality (21) also guarantees that thermal fluctuations of Z -ions around their WC positions are small. Therefore, F_{ZZ} can be written as

$$F_{ZZ} = \sum_{\mathbf{r}_i \neq 0} \frac{(Ze)^2}{D r_i} e^{-r_i/r_s}, \quad (22)$$

where the sum is taken over all vectors of WC lattice. At $r_s \ll R$, one needs to keep only interactions with the 6 nearest neighbours in Eq. (22). This gives

$$F = -\frac{2\pi\sigma r_s Z e n}{D} + 3n \frac{(Ze)^2}{DA} \exp(-A/r_s), \quad (23)$$

where $A = (2/\sqrt{3})^{1/2} n^{-1/2}$ is the lattice constant of this WC. Minimizing this free energy with respect to n one gets $A \simeq r_s \ln \zeta$, $R \simeq (2\pi/\sqrt{3})^{1/2} r_s \ln \zeta$ and

$$\frac{\sigma^*}{\sigma} = \frac{2\pi\zeta}{\sqrt{3} \ln^2 \zeta}, \quad (\zeta \gg 1). \quad (24)$$

It is clear from Eq. (24) that at $r_s \ll R$, or $\zeta \gg 1$ the distance R decreases and inverted charge continues to grow with decreasing r_s . This result could be anticipated for the toy model of Fig. 1a if the Coulomb interaction between the spheres is replaced by a strongly screened one. Screening obviously affects repulsion between positive spheres stronger than their attraction to the negative one and, therefore, makes it possible to keep two Z -ions even at $Q \ll Ze$.

Above we studied analytically two extremes, $r_s \gg R$ and $r_s \ll R$. In the case of arbitrary r_s we can find σ^* numerically. Indeed, minimizing the free energy (20) with the help of Eq. (22) one gets

$$\frac{1}{\zeta} = \sum_{\mathbf{r}_i \neq 0} \frac{3 + r_i/r_s}{8 r_i/r_s} e^{-r_i/r_s}, \quad (25)$$

where the sum over all vectors of WC lattice can be evaluated numerically. Using Eq. (25) one can find the equilibrium concentration n for any given value of ζ . The resulting ratio σ^*/σ is plotted by the solid curve in Fig. 5.

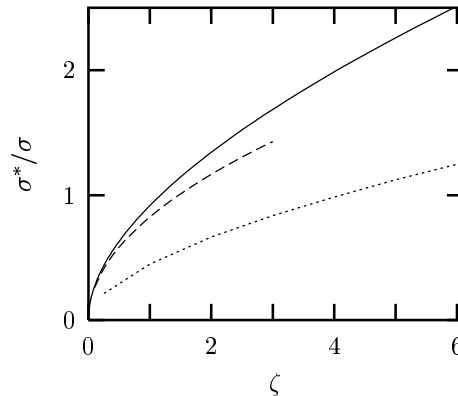


FIG. 5. The ratio σ^*/σ as a function of the dimensionless charge $\zeta = Ze/\pi\sigma r_s^2$. The solid curve is calculated for a charged plane by a numerical solution to Eq. (25), the dashed curve is the large r_s limit, Eq. (18). The dotted curve is calculated for the screening of the surface of the semispace with dielectric constant much smaller than 80. In this case image charges (Fig. 3b) are taken into account (See Sec. IV).

III. CONDENSATION OF MONOVALENT COIONS ON Z -ION. ROLE OF FINITE SIZE OF Z -ION.

We are prepared now to address the question of maximal possible charge inversion. How far can a macroion be overcharged, and what should one do to achieve that? We see below that to answer this questions one should take into account the finite size of Z -ions.

Fig. 5 and Eq. (24) suggest that the ratio σ^*/σ continues to grow with growing ζ . However, the possibilities to increase ζ are limited along with the assumptions of the presented theory. Indeed, there are two ways to increase $\zeta = Ze/\pi\sigma r_s^2$, namely to choose a surface with a small σ or to choose Z -ions with a large Z . The former way is restricted because, according to Eq. (21), Z -ion remains strongly bound to the charged plane only as long as $2\pi r_s \sigma Ze/D \gg k_B T s$ where

$$s = \ln(N_s/N) \quad (26)$$

is the entropy loss (in units of k_B) per Z -ion due to its adsorption to the surface. This gives for ζ :

$$\zeta \ll \zeta_{max} = 2Z^2 l_B / s r_s \quad (27)$$

Therefore, the latter way, which is to increase Z , is really the most important one. The net charge Z of a Z -ion is, however, restricted because at large charge Z_0 of the bare counterion monovalent coions of the charged plane (which have the sign opposite to Z -ions) condense on the Z -ion surface¹⁴. Assuming that Z -ions are spheres of the radius a , their net charge, Z , at large Z_0 can be found from the equation

$$Ze^2/aD = k_B T \ln(N_{1,s}/N_1), \quad (28)$$

where Ze^2/aD is the potential energy of a monovalent coion at the external boundary of the condensation atmosphere ("surface") of Z -ion and $k_B T \ln(N_{1,s}/N_1)$ is the difference between the chemical potentials of monovalent coions in the bulk and at the Z -ion's surface, $N_{1,s} \sim Z/a^3$ is the concentration of coions at the surface layer. Eq. (28) gives

$$Z = (2a/l_B) \ln(r_s/a). \quad (29)$$

Using Eq. (29) and Eq. (27), we arrive at

$$\zeta_{max} = \frac{8a^2}{sl_B r_s} \left[\ln \frac{r_s}{a} \right]^2, \quad (r_s \gg a). \quad (30)$$

In the theory presented in Sec. II, the radius of Z -ion, a , was the smallest length, even smaller than r_s . Therefore, the largest a we can substitute in Eq. (30) is $a = r_s$. For $r_s = a = 10\text{\AA}$ and $s = 3$ we get $\zeta_{max} \simeq 4$ so that the inversion ratio can be as large as 2.

Since charge inversion grows with increasing a we are tempted to explore the case $r_s \ll a \ll R_0$. To address this situation, our theory needs a couple of modifications. Specifically, in the first term of Eq. (23) we must take into account the fact that only a part of a Z -ion interacts with the surface, namely the segment which is within the distance r_s from the surface. Therefore, at $r_s \ll a$ results depend on the shape of ions and distribution of charge. If the bare charge of Z -ion is uniformly distributed on the surface of a spherical ion this adds small factor $r_s/2a$ to μ_{WC} and the right side of Eq. (27). This gives

$$\zeta_{max} = Z^2 l_B / sa \quad (31)$$

One should also take into account that at $a \gg r_s$ Eq. (29) should be replaced by

$$Z = a^2 / r_s l_B, \quad (32)$$

which follows from the condition that potential at the surface of Z -ion $Ze^2/aD - Ze^2/(a+r_s)D$ is equal to $k_B T \ln(N_{1,s}/N_1)$. Substituting Eq. (32) to Eq. (31) we find that ζ_{max} is larger than that given by Eq. (30), namely

$$\zeta_{max} = \frac{2a^3}{sl_B r_s^2}, \quad (r_s \ll a). \quad (33)$$

For $a = 20\text{\AA}$, $r_s = 10\text{\AA}$, $l_B = 7\text{\AA}$ and $s = 3$ we get $\zeta_{max} \simeq 8$ so that the inversion ratio can be as large as 3.

Let us consider now a special case of the compact Z -ion when it is a *short* rod-like polyelectrolyte of length $L < R$ and radius $a < r_s$. Such rods lay at the surface of macroion and form strongly correlated liquid reminding WC, so that one can still start from Eq. (27). In this case, however, Eqs. (29) and (32) should be replaced by $Z \sim L\eta_c/e = L/l_B$. Thus, $\zeta_{max} = 2R^2/sl_B r_s$ and can be achieved at $L \sim R$.

We conclude this section going back to spherical Z -ions and relatively weak screening. Until now we used everywhere the Debye-Hückel approximation for description of screening of surface charge density σ^* by monovalent salt. Now we want to verify its validity. Theory of Sec. II requires that the correlation voltage applied to capacitors $|\mu_{WC}|/Ze$ is smaller than $k_B T/e$. Using Eqs. (14) and (17) one can rewrite this condition as $Z < R/1.65l_B$. Substituting Z from Eq. (29) we find that one can use linear theory only when $r_s < r_m$, where

$$r_m = a \exp(R/3.3a). \quad (34)$$

For a large $R/2a$, the maximal screening radius of linear theory, r_m , is exponentially large. Nonlinear theory for $r_s > r_m$ is given in Sec. VII.

IV. SCREENING OF A THICK INSULATING MACROION BY SPHERICAL Z -IONS: ROLE OF IMAGES.

In Sec. II and III we studied a charged plane immersed in water so that screening charges are on both sides of the plane (Fig. 3a). In reality charged plane is typically a surface of a rather thick membrane whose (organic) material has the dielectric constant D_1 much less than that of water $D_1 \ll D$. It is well known in electrostatics that when a charge approaches the interface separating two dielectrics, it induces surface charge on interface. The potential created by these induced charges can be described as the potential of an image charge sitting on the opposite site of the interface (Fig. 3b). At $D_1 \ll D$,

this image charge has the same sign and magnitude as the original charge. Due to repulsion from images, Z -ions are pushed off the surface to some distance, d . One can easily find d in the case of a single Z -ion near the charged macroion in the absence of screening ($r_s = \infty$). The d -dependent part of the free energy of this system is

$$F = 4\pi\sigma Zed/D + (Ze)^2/4Dd. \quad (35)$$

Here the first term is the work needed to move Z -ion from the surface to the distance d , and the second term is the energy of image repulsion. The coefficient 4π (instead of 2π) in the first term accounts for the doubling of the plane charge due to the image of the plane. The ion sits at distance $d = d_0$ which minimizes the free energy of Eq. (35). Solving $\partial F/\partial d = 0$, one gets

$$d_0 = \frac{1}{4} \sqrt{\frac{Ze}{\pi\sigma}} = \frac{R_0}{4}. \quad (36)$$

In the presence of other counterions on the surface, the repulsive force is stronger, therefore one expects that d_0 is a little larger than $R_0/4$.

To consider the role of all images and finite r_s , let us start from the free energy per unit area describing the system:

$$F = -\frac{4\pi\sigma r_s Z e n}{D} e^{-d/r_s} + \frac{n}{2} \sum_{r_i \neq 0} \frac{(Ze)^2}{D r_i} e^{-r_i/r_s} + \frac{n}{2} \sum_{r_i} \frac{(Ze)^2}{D \sqrt{r_i^2 + 4d^2}} e^{-\sqrt{r_i^2 + 4d^2}/r_s}, \quad (37)$$

where, as in Eq. (22), the sums are taken over all vectors of the WC lattice. The four terms in Eq. (37) are correspondingly the self energy of the plane, the interaction between the plane and the Z -ions, the interaction between Z -ions (the factor $1/2$ accounts for the double counting), and the repulsion between Z -ions and the image charges (the factor $1/2$ accounts for the fact that electric field occupies only half of the space).

At large concentration of Z -ions in the bulk, the difference in the ideal parts of the free energy of Z -ion in solution and at the surface can be neglected, therefore, one can directly minimize the free energy (37) to find the concentration of Z -ions, n , at the surface and the optimum distance d . The system of equations

$$\frac{\partial F}{\partial d} = 0, \quad \frac{\partial F}{\partial n} = 0, \quad (38)$$

can be solved numerically and the results are plotted in Fig. 5. A remarkable feature of this plot is that, within 2% accuracy, the ratio σ^*/σ for the image problem is equal to a half of the same ratio for the charged plane immersed in water (for which there are no images). If we try to interpret this result using Eq. (14) of the capacitor model (Sec. II) we can say that image charges do not modify the "correlation" voltage $|\mu_{WC}|/Ze$. The

only substantial difference between two cases is that for the thick macroion, instead of charging two capacitors, one has to charge only one capacitor (on one side of the surface) with capacitance per unit area $D/4\pi r_s$.

The fact that image charges do not modify the "correlation voltage" can be explained quite simply in the case of weak screening $r_s \gg R_0$. In this limit, expanding the free energy (37) to the first order in d/r_s , we get

$$F = n\varepsilon(n) + \frac{n}{2} Ze\phi_{WC}(n, 2d) + \frac{2\pi\sigma^2 d}{D} + \frac{2\pi(\sigma^*)^2 r_s}{D}. \quad (39)$$

The physical meaning of this equation is quite clear. The first two terms are energies of the WC and of its interaction with the image WC ($\phi_{WC}(n, 2d)$ is the potential of a WC with charge density Zen at the location of an image of Z -ion.) The third term is the capacitor energy created by the charge of WC and the plane charge. And the final term is the usual energy of a capacitor made by the WC and the screening atmosphere.

At $\sigma^*/\sigma \ll 1$ minimization of Eq. (39) with respect to d gives the optimum distance $d_0 = 0.3R_0$, which is a little larger than the estimate (36). Minimization with respect to n gives an equation similar to Eq. (14)

$$\sigma^* = \frac{D}{4\pi r_s} \frac{|\mu_{WC}|}{Ze}, \quad (40)$$

where μ_{WC} differs from the corresponding value in the case of immersed plane (Eq. (17)) only by:

$$\delta\mu_{WC} = \frac{\partial}{\partial n} \left[\frac{n}{2} Ze\psi_{WC}(n, 2d_0) \right]. \quad (41)$$

It is known that $\psi_{WC}(x)$ decreases exponentially with x when $x > A/2\pi$. Since $2d_0/(A/2\pi) \simeq 1.8$, the potential $\psi_{WC}(n, 2d_0) \propto \exp(-2d_0 \cdot 2\pi/A)$ and $\delta\mu_{WC}/|\mu_{WC}| \simeq (1 - d_0 \frac{2\pi}{A}) \exp(-2d_0/(A/2\pi)) \simeq 0.02$. Thus, at $r_s \gg R_0$ the chemical potential μ_{WC} remains practically unchanged by image charges.

In the opposite limit $r_s \ll R_0$ one can calculate the ratio σ^*/σ by direct minimization of the free energy, without the use of the capacitor model. Keeping only the nearest neighbour interactions in Eq. (37) one finds

$$d_0 = r_s \ln \frac{\zeta}{8},$$

$$\frac{\sigma^*}{\sigma} \simeq \frac{2\pi\zeta}{\sqrt{3} \ln^2(\zeta^2/10(d/r_s))} \simeq \frac{\pi\zeta}{2\sqrt{3} \ln^2 \zeta}. \quad (42)$$

Comparing this result with Eq. (24) for the case of immersed plane (no image charges), one gets

$$\frac{(\sigma^*/\sigma)_{image}}{(\sigma^*/\sigma)_{no\ image}} = \frac{1}{4} \left[1 + \frac{\ln 10}{\ln \zeta} \right]. \quad (43)$$

Eq. (43) shows that in the limit $\zeta \rightarrow \infty$, the ratio σ^*/σ for the image problem actually approaches $1/4$ of

that for the problem without image. However, due to the logarithmic functions, it approaches this limit very slowly. Detailed numerical calculations show that even at $\zeta = 1000$, the ratio (43) is still close to 0.5. In practice, ζ can hardly exceed 20, and this ratio is always close to 0.5 as Fig. 5 suggested.

Although at a given ζ , image charges do not change the results qualitatively, they, as we show below, reduce the value of ζ_{max} substantially. As in Sec. III, we find ζ_{max} from the condition that the bulk electrochemical potential of Z -ions can be neglected. When images are present, according to Eq. (37), one need to replace the right hand side of Eq. (21) by $2\pi\sigma r_s Z e \exp(-d_0/r_s)$. Using Eq. (42), this condition now reads

$$\zeta \ll \zeta_{max} = 4\sqrt{Z^2 l_B / sr_s} \quad (44)$$

Using Eq. (44) instead of Eq. (27) and using Eq. (29) for Z we get $\zeta_{max} \simeq 5$ at $r_s = a = 10\text{\AA}$ and $s = 3$. Therefore, according to the dotted curve of Fig. 5 which was calculated for the case of image charges, the inversion ratio for a thick macroion can be as large as 100%.

V. LONG CHARGED RODS AS Z -IONS. STRONG SCREENING BY MONOVALENT SALT.

As we mentioned in Introduction the adsorption of long rod-like Z -ions such as DNA double helix on an oppositely charged surface leads to the strong charge inversion. In this case, correlations between rods cause parallel ordering of rods in a strongly correlated nematic liquid. In other words, in the direction perpendicular to the rods we deal with short range order of one-dimensional WC (Fig. 4).

Consider the problem of screening of a positive plane with surface charge density, σ , by negative DNA double helices with the net linear charge density $-\eta$ and the length L smaller than the DNA persistence length L_p so that they can be considered straight rods. For simplicity, the charged plane is assumed to be thin and immersed in water so that we can neglect image charges. Modification of the results due to image charges is given later. Here, the strong screening case $r_s \ll A$ is considered (A is the WC lattice constant). The weak screening case, $r_s \gg A$, is the topic of the next section.

We show below that at $r_s \ll A$ screening radius r_s is smaller than the Gouy-Chapman length for the bare plane. Therefore, one can use Debye-Hückel formula, $\psi(0) = 2\pi\sigma r_s / D$, for the potential of the plane. On the other hand, the "bare" surface charge of DNA is very large, and its corresponding Gouy-Chapman length is much smaller than r_s . As the result, one needs nonlinear theory for description of the net charge of DNA. It leads to Onsager-Manning conclusion that positive monovalent ions condense on the surface of DNA reducing its net charge, $-\eta$, to $-\eta_c = -Dk_B T / e$. Far away from DNA, the linear theory can be used. When DNA rods

condense on the plane, we can still use $-\eta_c$ as the net charge density of DNA, because as we will see later, the strongly screened potential of plane only weakly affects condensation of monovalent ions on DNA.

Therefore, we can write the free energy per DNA as

$$f = -\frac{2\pi\sigma r_s L \eta_c}{D} + \frac{1}{2} \sum_{\substack{i=-\infty \\ i \neq 0}}^{\infty} \frac{2L\eta_c^2}{D} K_0\left(\frac{iA}{r_s}\right), \quad (45)$$

where $K_0(x)$ is the modified Bessel function of 0-th order. The first term of Eq. (45) describes the interaction energy of DNA rods with the charged plane, the second term describes the interaction between DNA rods arranged in one-dimensional WC, the factor 1/2 accounts for the double counting of the interactions in the sum.

Since the function $K_0(x)$ exponentially decays at large x , at $r_s \ll A$ one can keep only the nearest neighbour interactions in Eq. (45). This gives

$$f \simeq -\frac{2\pi\sigma r_s L \eta_c}{D} + \frac{2L\eta_c^2}{D} \sqrt{\frac{\pi r_s}{2A}} \exp(-A/r_s), \quad (46)$$

which is similar to Eq. (23). To find A , we minimize the free energy per unit area, $F = nf$, with respect to n , where $n = 1/LA$ is the concentration of DNA helices at the charged plane. This yields:

$$\frac{\sqrt{2\pi\sigma r_s}}{\eta_c} = \sqrt{A/r_s} \exp(-A/r_s). \quad (47)$$

Calculating the net negative surface charge density, $-\sigma^* = -\eta_c/A + \sigma$, we obtain for the inversion ratio

$$\frac{\sigma^*}{\sigma} \simeq \frac{\eta_c / \sigma r_s}{\ln(\eta_c / \sigma r_s)} \quad (r_s \ll A). \quad (48)$$

As we see from Eq. (47), the lattice constant A of WC decreases with decreasing r_s and charge inversion becomes stronger.

Let us now address the question of the maximal charge inversion in the case of screening by DNA. Similar to what was done in Sec. III, the charge inversion ratio is limited by the condition that the electrochemical potential of DNA in the bulk solution can be neglected and therefore, DNA is strongly bound to the surface. Using Eq. (46) and (47), this condition can be written by an equation similar to Eq. (21)

$$k_B T s \ll 2\pi\sigma r_s L \eta_c / D \quad \text{or} \quad \eta_c / \sigma r_s \ll 2\pi L / s l_B, \quad (49)$$

where $s = \ln(N_{s,DNA}/N_{DNA})$ is the entropy loss (in units of k_B) per DNA due to its adsorption to the surface. $N_{s,DNA}$ and N_{DNA} are correspondingly the three-dimensional concentration of DNA at the charged surface and in the bulk. Inequality (49) also guarantees that WC-like short range order of DNA helices is preserved. To show this, let us assume that the left and right nearest neighbour rods at the surface are parallel to each other

and discuss the amplitude of the thermal fluctuations of the central DNA along the axis x perpendicular to DNA direction (in the limit $r_s \ll A$, we need to deal only with two nearest neighbours of the central DNA). At $x = 0$, the free energy of the rod is given by Eq. (46). At $x \neq 0$ the free energy of the central DNA is

$$f(x) \simeq -\frac{2\pi\sigma r_s \eta_c L}{D} + \frac{2L\eta_c^2}{D} \sqrt{\frac{\pi r_s}{2A}} \cosh\left(\frac{x}{r_s}\right) e^{-A/r_s}. \quad (50)$$

Using Eqs. (50) and (47), we find the average amplitude, x_0 , of the fluctuations of x from the condition $f(x_0) - f(0) \simeq k_B T$. This gives $x_0 \simeq r_s \ln(Ae/2\pi\sigma r_s^2 L)$. The inequality (49) then gives:

$$x_0 < r_s \ln \frac{A}{r_s} \simeq r_s \ln \ln \frac{\eta_c}{\sigma r_s} \ll A \simeq r_s \ln \frac{\eta_c}{\sigma r_s}. \quad (51)$$

Thus, DNA helices preserve WC-like short range order when the condition (49) is met.

This condition obviously puts only a weak restriction on maximum value of σ^*/σ . At $L = L_p = 50$ nm and $s = 3$, the parameter $\eta_c/\sigma r_s$ can be as large as 75 and, according to Eq. (48) the ratio σ^*/σ can reach 15. Therefore, we can call this phenomenon *strong charge inversion*.

This limit can be easily reached at a very small σ . On the other hand, if we want to reach it making r_s very small we have to modify this theory for the case when r_s is smaller than the radius of DNA. In a way, this is similar to what was done in Sec. 3 for spherical Z -ions. At $r_s \ll a$ one replaces the net charge of DNA, η_c by $\eta_c a/r_s$ and adds small factor $(r_s/\pi^2 a)^{1/2}$ to the first term of Eq. (46). This modification changes only logarithmic term of Eq. (48) and does not change our conclusion about strong charge inversion.

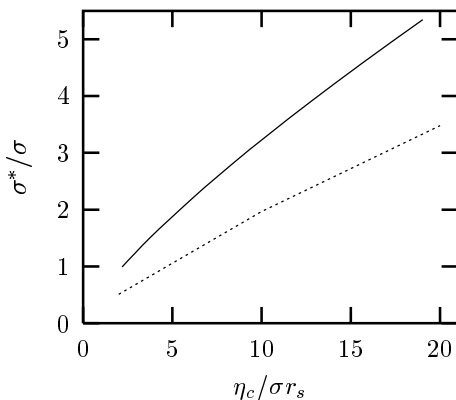


FIG. 6. The ratio σ^*/σ as a function of $\eta_c/\sigma r_s$. The solid curve is calculated for a charged plane by numerical solution to Eq. (45). The dotted curve is calculated for the screening of the surface of the semi-space with dielectric constant much smaller than 80. In this case image charges are taken into account.

One can numerically minimize the free energy (45) at all $r_s \leq A$ to find σ^*/σ . The result is plotted by the solid curve in Fig. 6.

Let us now move to the more realistic case of a thick macroion, so that repulsion from image charges must be taken into consideration. As in the spherical Z -ion case, image charges push the WC off the surface to some distance d . The free energy per DNA rod can be written as

$$f = -\frac{4\pi\sigma r_s L \eta_c}{D} e^{-d/r_s} + \frac{1}{2} \sum_{i=-\infty}^{\infty} \frac{2L\eta_c^2}{D} K_0\left(\frac{iA}{r_s}\right) + \frac{1}{2} \sum_{i=-\infty}^{\infty} \frac{2L\eta_c^2}{D} K_0\left(\frac{\sqrt{(iA)^2 + 4d^2}}{r_s}\right), \quad (52)$$

where the three terms on the right hand side are correspondingly the interaction between the plane and the DNA, between the different DNAs and between the DNAs and their images.

The equilibrium distance d_0 and A can be obtained by minimizing the free energy per unit area $F = nf$ with respect to d and $n = 1/LA$:

$$\frac{\partial F}{\partial d} = 0, \quad \frac{\partial F}{\partial n} = 0, \quad (53)$$

This system of equations is solved numerically. The result for σ^*/σ is plotted by the dotted curve in Fig. 6. It is clear that in the case of DNA, at a given value of $\eta_c/\sigma r_s$, image charges play even smaller role than for spherical Z -ions. The ratio σ^*/σ in the case of a thick macroion is close to 70% of σ^*/σ for the charged plane immersed in water, instead of 50% as in Fig. 5 for spherical Z -ions.

However, like in the case of spherical Z -ions, image charges modify the maximal possible value of $\eta_c/\sigma r_s$ significantly. When images are present, according to Eq. (52), one need to replace in Eq. (49) $2\pi\sigma r_s L \eta_c/D$ by $2\pi\sigma r_s L \eta_c \exp(-d_0/r_s)$. Therefore, the condition that the bulk ideal chemical potential can be neglected and, therefore, DNA is strongly bound at the surface has the form

$$k_B T s \ll 2\pi\sigma r_s L \eta_c \exp(-d_0/r_s). \quad (54)$$

Similarly to what was done above for the problem of charged plane immersed in water one can show that Eq. (54) guarantees, also, WC-like short range order of DNA helices. In the limit $\eta_c \gg \sigma r_s$, keeping only the nearest neighbour interactions in the free energy (52) and minimizing with respect to d one gets $d_0 \simeq r_s \ln(\eta_c/4\sigma r_s)$. Substituting d_0 into Eq. (54) we arrive at the final form for the condition of Eq. (49):

$$\eta_c/\sigma r_s \ll \sqrt{8\pi L/sl_B}, \quad (L \leq L_p). \quad (55)$$

It is clear that the maximal $\eta_c/\sigma r_s$ and maximal inversion ratio grow with L . For $L = L_p = 50$ nm and $s = 3$, the

maximal $\eta_c/\sigma r_s = 25$. Therefore, according to the dotted curve in Fig. 6, the inversion ratio for a thick macroion σ^*/σ can reach 4. Such inversion can still be considered as strong.

Until now we talked about relatively short DNA, $L \leq L_p$, which can be considered as a rod. For DNA double-helices of a larger length ($L \gg L_p$) the maximum inversion ratio saturates at the value obtained above at $L = L_p$. This happens because even a long DNA can not be adsorbed at the surface if for $L = L_p$ inequality (55) is violated. (See the theory of adsorption-desorption phase transition, for example, in Ref. 21).

On the other hand, if inequality (55) holds at $L = L_p$, i. e. at $\eta_c/\sigma r_s \ll \sqrt{8\pi L_p/s}l_B$, the adsorption of a long DNA is so strong that DNA lays flat on the charged surface. Since repulsion between neighbouring parallel DNA is balanced with attraction to the surface, interactions between parallel DNA helices are so strong that the same inequality guarantees WC-like short range order at the length scale L_p , even though DNA length is much larger than L_p . One can verify this statement studying lateral fluctuations of a DNA segment with length L_p similarly to the calculation presented above for the problem of charged plane immersed in water (See Eqs. (50) and (51)). Thus, our theory and the plots of Fig. 5 are applicable for a long DNA and, therefore, for any flexible polyelectrolyte.

To conclude this section, we would like to mention another charge inversion problem similar to the problem we considered here. Giant charge inversion can be also achieved if a single very long DNA double helix screens a long and wide positively charged cylinder with radius greater or about the double helix DNA persistence length (Fig. 7).

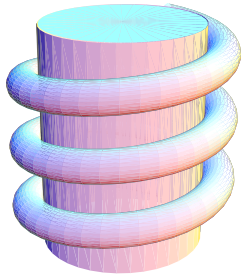


FIG. 7. A long charged worm-like rods spirals around an oppositely charged cylinder to screen it. Locally, the picture resembles that of an one-dimensional WC

In this case, an DNA double helix spirals around the cylinder. Neighbouring turns repel each other so that DNA forms an almost perfect coil which locally resembles one-dimensional WC. As a result, the cylinder charge inverts its sign: density of DNA charge per unit length of the cylinder becomes larger than the bare linear charge density of the cylinder. At small r_s this charge inver-

sion can be as strong as we discussed above. If cylinder diameter is smaller than DNA persistent length one should add elastic energy to the minimization problem. This, of course, will make charge inversion weaker than for wider cylinders, but still it can be quite large. We leave open the possibility to speculate on the relevance of these model systems to the fact that DNA overcharges a nucleosome by about 15%⁴.

A similar problem of wrapping of a *weakly* charged polyelectrolyte around oppositely charged sphere was recently studied in the Debye-Hückel approximation in Ref. 7. A strong charge inversion was found in this case as well. Charge inversion for a charged sphere screened by an oppositely charged flexible polyelectrolyte was previously observed in experiment⁸ and numerical simulations⁹.

VI. LONG CHARGED RODS AS Z-IONS. WEAK SCREENING BY MONOVALENT SALT

In this section, we consider screening of a positively charged plane by DNA rods in the case of weak screening, when $r_s \gg A$. We saw in Sec. II that when the screening radius is larger than the lattice constant of WC, the capacitor model provides a transparent description of the charge inversion. Here we adopt this model, too. However, we find out that in the case of rods, the inversion charge σ^* is so large that its screening by monovalent salt is nonlinear. In other words, at $r_s \gg A$, the capacitors described in Sec. II becomes nonlinear. Correspondingly in this case one has to use the solution of the nonlinear PB equation for the plane potential:

$$\psi(0) \simeq -(2k_B T/D_e) \ln(r_s/\lambda). \quad (56)$$

where $\lambda = e/\pi\sigma^*l_B$ is the Gouy-Chapman length. It is shown below that $A \ll \lambda \ll r_s$ so that the use of Eq. (56) is justified.

The weak screening of the plane potential has also another important consequence. The net charge density of DNA, $-\eta$, ceases to be equal to to the Onsager-Manning critical density $-\eta_c$. The charge of the plane forces DNA to release some of monovalent coions condensed on it, so that η becomes larger than η_c . Thus, in this case, we have to deal with a nonlinear problem with two unknowns, η and σ^* .

One can find these unknowns from the two following physical conditions of equilibrium. The first one requires that the chemical potential of positive monovalent ions (coions) in the bulk of solution is equal to the chemical potential of coions condensed on the surface of DNA rods which, in turn, are adsorbed on the plane. The second condition requires that the chemical potentials for DNA rods in the bulk solution and DNA rods of the surface WC are equal. Let us write the first condition as

$$k_B T \ln \frac{N_{1,s}}{N_1} = -e\psi(0) + \frac{2e\eta}{D} \ln(A/2\pi a), \quad (57)$$

where N_1 and $N_{1,s}$ are the concentrations of monovalent coion in the bulk and at the DNA surface respectively. The left-hand side of Eq. (57) is the entropy loss and the right-hand side is the potential energy gain when monovalent salt condenses on the DNA surface (the potential at the surface of DNA is the sum of $\psi(0)$, of the nonlinear plane capacitor made and the potential of the DNA charged cylinder with radius a and the linear charge density $-\eta$, screened at the distance $A/2\pi$, by neighbouring DNA). Far from the charged plane, DNA net charge regains its value $-\eta_c$, the condition of equilibrium of condensed monovalent coions on isolated DNA rod with those in the bulk can be written in a way similar to Eq. (57):

$$k_B T \ln \frac{N_{1,s}}{N_1} = \frac{2e\eta_c}{D} \ln \frac{r_s}{a}. \quad (58)$$

Excluding $\ln(N_{1,s}/N_1)$ from Eqs. (57) and (58) and using Eq. (56) we can write the first equation for λ (which represents σ^*) and η as

$$\eta_c \ln \frac{r_s}{a} = \eta_c \ln \frac{r_s}{\lambda} + \eta \ln \frac{A}{2\pi a}. \quad (59)$$

The equality of the chemical potential of DNA in the bulk and of DNA condensed on the plane can be written in the form similar to Eq. (14)

$$L\eta\psi(0) = |\mu_{WC}| + \frac{L\eta - L\eta_c}{e} k_B T \ln \frac{N_{1,s}}{N_1} - \left(\frac{L\eta^2}{D} \ln \frac{\lambda}{a} - \frac{L\eta_c^2}{D} \ln \frac{r_s}{a} \right). \quad (60)$$

As in Eq. (14), we see that a "correlation voltage", $|\mu_{WC}|/L\eta$, charges two capacitors consisting of the overcharged plane and its screening atmosphere to a finite voltage $\psi(0)$. The new second and third terms on the right hand side are due to the change in the net charge of DNA, when it condenses on the plane. Specifically, the second term is the gain in the entropy of monovalent salt released and the third term is the loss in the self energy of DNA when its net charge changes from $-\eta_c$ in the bulk solution to $-\eta$ at the plane surface. Here λ is the screening length near the plane surface. (This can be seen from the fact that the three-dimensional concentration of monovalent salt at the surface is of the order $N_{1,s} \sim \sigma^*/2e\lambda$ and the corresponding screening length $r_{s,surf} = (4\pi N_{1,s} l_B)^{-1/2} \sim (2\lambda e/\pi\sigma^* l_B)^{1/2} \sim \lambda$.)

A formal derivation of Eq. (60) is given in the end of this section.

The free energy per DNA of the one-dimensional WC of DNA rods at the surface can be written similarly to Eq. (45) with the screening length r_s replaced by λ ,

$$f = -\frac{2\pi(\eta/A)\lambda}{D} L\eta + \frac{1}{2} \sum_{i=-\infty, i \neq 0}^{\infty} L\eta \frac{2\eta}{D} K_0 \left(\frac{iA}{\lambda} \right) \simeq -\frac{L\eta^2}{D} \ln \frac{2\pi\lambda}{A}. \quad (61)$$

This result can be interpreted as the interaction of DNA with its Wigner-Seitz cell (a stripe with length L , width A and charge density η/A).

The chemical potential μ_{WC} can be easily calculated:

$$\mu_{WC} = \frac{\partial[nf]}{\partial n} \simeq -\frac{L\eta^2}{D} \ln \frac{2\pi\lambda}{A}, \quad (62)$$

where $n = 1/LA$ is the concentration of DNA at the charged surface.

Substituting Eqs. (56), (58), and (62) into Eq. (60), we arrive at the second equation for η and λ

$$2\eta\eta_c \ln \frac{r_s}{\lambda} = -\eta_c^2 \ln \frac{r_s}{a} - \eta^2 \ln \frac{A}{2\pi a} + 2\eta_c\eta \ln \frac{r_s}{a}. \quad (63)$$

Solving Eqs. (59) and (63) together with $A = \eta/(\sigma + \sigma^*)$, we get

$$\eta \simeq \eta_c \sqrt{\frac{\ln(r_s/a)}{\ln(A_0/2\pi a)}}, \quad (64)$$

$$\ln \frac{\lambda}{a} \simeq \sqrt{\ln \frac{r_s}{a} \ln \frac{A_0}{2\pi a}}, \quad (65)$$

where $A_0 = \eta_c/\sigma$.

Eq. (65) shows that the theory is self consistent: when $r_s \gg A_0$, one has $r_s \gg \lambda \gg A_0$. This justifies the use of nonlinear potential for the plane. Eq. (64) demonstrates that $\eta \gg \eta_c$ as we anticipated. Eq. (64), of course, is valid only if $\eta \leq \eta_0$, where η_0 is bare linear charge density of DNA.

The ratio σ^*/σ can now be easily calculated by substituting $\lambda = e/\pi\sigma^* l_B$ into Eq. (65). One arrives at Eq. (6) which shows that the ratio σ^*/σ increases as r_s decreases, but remains smaller than unity. When $r_s \sim A_0$ one finds from Eqs. (64) and (65) that $\eta \sim \eta_c$, $\lambda \sim r_s \sim A_0$, and $\sigma^*/\sigma \sim 1$, what matches the Eq. (48) obtained for the strong screening limit ($r_s \ll A$).

Let us now present a derivation of Eq. (60). To calculate the free energy of the system we use the standard charging procedure described, for example, in Ref. 22 and used for DNA in Ref. 23,24. First, let us start by calculating the electrostatic free energy of a DNA dissolved in solution, which can be written as the work needed to charge the DNA up to the bare value η_0 per unit length

$$f = L \int_0^{\eta_0} \phi(\eta') d\eta', \quad (66)$$

where $\phi(\eta')$ is the self consistent surface potential of DNA when its charge is η' per unit length. Following Ref. 24, let us divide this charging process in two steps. First, the DNA is charged from 0 up to η_c . In this step, one can use for $\phi(\eta')$ the linear (Debye-Hückel) potential

$$\phi(\eta') = \frac{2\eta'}{D} \frac{K_0(a/r_s)}{K_1(a/r_s)a/r_s} \simeq \frac{2\eta'}{D} \ln(r_s/a), \quad (r_s \gg a). \quad (67)$$

In the next step, DNA is charged from η_c to η . In this step, one has to use nonlinear potential for $\phi(\eta')$. It can be written as a sum

$$\phi(\eta') = 2 \frac{k_B T}{De} \ln \frac{a}{\Lambda(\eta')} + \frac{2\eta_c}{D} \ln \frac{r_s}{a}, \quad (68)$$

where the first term is the contribution of the interval $2a > r > a$ of the distances r from the DNA axis. In this interval potential can be approximated by that of the charged plane with charge density $\eta'/2\pi a$. It has Gouy-Chapman form with the corresponding Gouy-Chapman length $\Lambda(\eta') = a\eta_c/\eta' < a$. The second term in Eq. (68) is the contribution of interval $\infty > r > 2a$, where we deal with a cylinder of radius a and linear net charge density $-\eta_c$. Now, we can calculate the free energy of a DNA rod (which is also the chemical potential of DNA in the bulk solution, apart from an ideal part):

$$\begin{aligned} f &= L \int_0^{\eta_c} \phi(\eta') d\eta' + L \int_{\eta_c}^{\eta_0} \phi(\eta') d\eta' \\ &= \frac{L\eta_c^2}{D} \ln \frac{r_s}{a} + \frac{L2\eta_c\eta_0}{D} \ln \frac{a}{\Lambda(\eta_0)} + \frac{L2\eta_c}{D} (\eta_0 - \eta_c) \ln \frac{r_s}{a}. \end{aligned} \quad (69)$$

In the Onsager-Manning condensation theory, one can think of the last two terms in the above expression as the free energy of the condensation layer.

When DNA rods are adsorbed on the surface of the macroion, the role of η_c as a border between the linear and nonlinear charging regime is played by the net charge η . We calculate the total free energy of the system by first charging the plane surface to σ and DNA to η respectively, then continue charging the DNA from η to the final value η_0 . The first charging process leads to the standard contribution

$$L\eta\psi(0) + \mu_{WC} + \frac{L\eta^2}{D} \ln \frac{\lambda}{a},$$

to the chemical potential of DNA, where the three terms result from, correspondingly, the capacitor energy of the screening atmosphere, the correlation energy of DNA and the self energy of DNA. The second charging process builds up the condensation layer around each DNA and gives a contribution

$$\int_{\eta}^{\eta_0} \phi(\eta) d\eta = \frac{2\eta_c\eta_0}{D} \ln \frac{a}{\Lambda(\eta_0)} + \frac{2\eta_c}{D} (\eta_0 - \eta) \ln \frac{r_s}{a}$$

where the nonlinear potential of Eq. (68) was used.

The chemical potential of DNA on the charged surface is the sum of the two above contributions:

$$\begin{aligned} L\eta\psi(0) + \mu_{WC} + \frac{L\eta^2}{D} \ln \frac{\lambda}{a} + \frac{L2\eta_c\eta_0}{D} \ln \frac{a}{\Lambda(\eta_0)} \\ + \frac{L2\eta_c}{D} (\eta_0 - \eta) \ln \frac{r_s}{a}. \end{aligned} \quad (70)$$

Equating this expression to the chemical potential of DNA in the bulk (Eq. (69)) one gets the desired Eq. (60).

So far, we have dealt only with the screening of charged surface by DNA double helices which are highly charged polyelectrolytes. The situation is simpler if one deals with weakly charged polyelectrolytes whose bare charge density η_0 is much smaller than η_c . In this case, there is no condensation on the polyelectrolyte. Therefore η_0 plays the role of the net charge η_c . In the weak screening case, $r_s \gg \eta_0/\sigma$, this brings about small changes in Eq. (60), which now reads:

$$L\eta_0\psi(0) = |\mu_{WC}| - \left(\frac{L\eta_0^2}{D} \ln \frac{\lambda}{a} - \frac{L\eta_0^2}{D} \ln \frac{r_s}{a} \right). \quad (71)$$

Substituting Eq. (56) and (62) into Eq. (71), and solving for λ , we get

$$\lambda \simeq r_s \exp \left(\frac{\eta_0}{\eta_c} \ln \frac{\eta_0}{\sigma r_s} \right) \quad (r_s \gg \eta_0/\sigma). \quad (72)$$

Nonlinear effects are important when $\lambda \ll r_s$, or when the exponent in the above expression becomes less than -1 . This gives the minimal r_s at which nonlinear effects are still important.

$$r_m = (\eta_0/\sigma) \exp(\eta_c/\eta_0). \quad (73)$$

As we see, r_m is exponentially large at $\eta_c/\eta_0 \gg 1$. This makes this weak screening case practically unimportant. At smaller, more realistic value of r_s , one can use Debye-Hückel linear theory to describe the potential of the plane. For $r_s < \eta_0/\sigma$, this has been done in Ref. 6. The result is an expression similar to Eq. (48) with the net charge η_c replaced by the bare charge η_0 .

VII. NONLINEAR SCREENING OF A CHARGED SURFACE BY SPHERICAL Z-IONS.

Let us now return to the screening of the charged plane by spherical Z -ions in the case when screening by monovalent salt is very weak. Our goal is to understand what happens when screening radius is larger than r_m (see Eq. (34)), so that Debye-Hückel approximation of Sec. II for the description of screening of surface charge density σ^* by monovalent salt fails and a nonlinear description is necessary.

The nonlinearity of screening leads to two important changes in the theory in Sec. II. First, the monovalent coions condense on the surface of the Z -ion and reduce its apparent charge. We discussed this condensation in Sec. III, but used for the net charge of Z -ion the value obtained for isolated Z -ion in the bulk solution (Eq. (28)).

In this section we call this charge Z_c (this quantity plays a similar role as η_c in previous section) and save notation Z for the net charge of Z -ion adsorbed at the charged surface as a part of the WC. When positive Z -ions condense on the negative surface, a fraction of monovalent negative ions, condensed on the Z -ions is released. Therefore, strictly speaking, $Z > Z_c$. The charge Z_c can be found from Eq. (28), which in the revised notation reads

$$e \frac{Z_c e}{aD} = k_B T \ln \frac{N_{1,s}}{N_1}. \quad (74)$$

Here, as in Sec. III, $N_{1,s}$ is the concentration of monovalent negative ions at the external boundary of the condensation atmosphere of the isolated spherical Z -ion. The net charge of a Z -ion in WC, Z , can be found from the condition of equilibrium of monovalent negative ions condensed on a Z -ion of the WC and those in the bulk solution

$$\frac{Z e^2}{aD} - e \left(\frac{2.2 Z e}{RD} + \psi(0) \right) = k_B T \ln \frac{N_{1,s}}{N_1}. \quad (75)$$

The term in the parentheses is the total potential of the plane and other adsorbed Z -ions at the considered Z -ion. This potential is the sum of the negative potential of WC and the potential due to the positive net charge σ^* of the plane given by Eq. (56). Excluding $k_B T \ln(N_{1,s}/N_1)$ from Eqs. (74) and (76) we obtain the first equation for two unknowns Z and λ , which is similar to Eq. (59):

$$\frac{Z e^2}{aD} - \frac{2.2 Z e^2}{RD} + 2k_B T \ln(r_s/\lambda) = \frac{Z_b e^2}{aD}. \quad (76)$$

To write the second equation for these unknowns we start from the condition that the chemical potentials of Z -ion at the charged surface and in the bulk solution are equal. In the close analogy with Eq. (60) of Sec. VI, we can write

$$Z e \psi(0) = |\mu_{WC}| + (Z - Z_c) k_B T \ln \frac{N_{1,s}}{N_1} + \frac{(Z_b^2 - Z^2) e^2}{2aD}. \quad (77)$$

The second and third terms on the right-hand side account for the fact that monovalent ions are released when Z -ions condense on the plane surface (so that their entropy is gained) and simultaneously the self energy of the Z -ion is reduced. Using Eqs. (17), (56) and (74) we obtain the second equation for Z and λ

$$2k_B T Z \ln \frac{r_s}{\lambda} = \frac{1.65(Ze)^2}{RD} + \frac{(Z - Z_c) Z_b e^2}{aD} + \frac{(Z_b^2 - Z^2) e^2}{2aD}. \quad (78)$$

Solving Eqs. (76) and (78) we get

$$\frac{Z}{Z_c} \simeq 1 + \frac{0.56 a}{R} \quad (79)$$

and

$$\lambda = r_s \exp \left(-\frac{1.65a}{2R} \ln \frac{N_{1,s}}{N_1} \right). \quad (80)$$

Approximating $N_{1,s}$ as $N_{1,s} \sim Z/a^3$, we get

$$\ln \frac{N_{1,s}}{N} = 2 \ln \frac{r_s}{a}.$$

Therefore

$$\lambda = r_s \exp \left(-\frac{1.65a}{R} \ln \frac{r_s}{a} \right). \quad (81)$$

Nonlinear effects are important when $\lambda \ll r_s$, or when the exponent in the above expression becomes less than -1 . This gives the minimal r_s at which nonlinear effects are still important

$$r_m = a \exp(R/1.65a), \quad (82)$$

which matches the estimate Eq. (34) obtained from the side of the linear regime.

The ratio σ^*/σ can be easily calculated from Eq. (80)

$$\begin{aligned} \frac{\sigma^*}{\sigma} &= \frac{e}{\pi \sigma l_B r_s} \exp \left(-\frac{1.65a}{R} \ln \frac{r_s}{a} \right) \\ &= \frac{e}{\pi \sigma l_B r_s} \left(\frac{r_s}{a} \right)^{-1.65a/R} \propto r_s^{-(1+1.65a/R)}. \end{aligned} \quad (83)$$

Once again, this ratio increases as r_s decreases²⁵. Comparing Eq. (83) to Eq. (18), we see that nonlinear effects change the exponent in the dependence of σ^*/σ on r_s by $1.65a/R \ll 1$. Taking into account the fact that it is important only when r_s is greater than an exponentially large critical value r_m (see Eq. (82)), one can conclude from this section that, in practical situation, non-linear effects in the problem of screening of a charged surface by spherical Z -ions are not important.

VIII. SCREENING OF A MACROION WITH A MOBILE SURFACE CHARGE.

So far we have assumed that the bare surface charges of the macroion are fixed and can not move. For solid or glassy surfaces, colloidal particles and even rigid polyelectrolytes, such as double helix DNA and actin, this approximation seems to work well. On the other hand, for charged lipid membranes it can be violated. The membrane can have a mixture of neutral and, for example, negatively charged hydrophilic heads. In a liquid membrane heads are mobile so that negative ones can accumulate near the positive Z -ion and push the neutral heads outside (see Fig. 8). Since the background charges are now closer to the counterion, one can immediately predict that the energy of the WC is lower and charge

inversion is stronger than that for the case of an uniform distribution of negative heads.

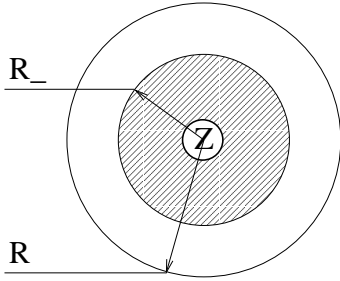


FIG. 8. A Z -ion and its Wigner-Seitz cell with radius R are shown. The negative heads are concentrated in the shaded area with radius R_- . The rest of the Wigner-Seitz cell is occupied by the neutral ones.

To simplify the calculation of the free energy, and gain more physical insight in the problem, let us use the same transformation as in the beginning of section II, namely we simultaneously add uniform planar charge densities $-\sigma^*$ and σ^* to the plane. The first addition makes a neutral WC on the plane. While the second addition creates the two planar capacitors. The free energy can be written as the sum of the energy of WC and two capacitors, in the same way as Eq. (9). Therefore, σ^* is given by Eq. (14).

We use below the Wigner-Seitz approximation to calculate μ_{WC} . This approximation gives the energy per ion of WC as the energy of one Wigner-Seitz cell and neglects the quadrupole-quadrupole interaction between Wigner-Seitz cells. It provides 5% accuracy for the energy of the standard WC on an uniform immobile background (see Eq. (16)). In the case of mobile charges, as one sees from Fig. 7, the quadrupole moment of the Wigner-Seitz cell is even smaller than that for WC on an uniform background with the same average charge density σ . Therefore, in the case of mobile charge, the accuracy of the Wigner-Seitz approximation is even better.

For simplicity, we assume the Wigner-Seitz cell of a counterion is a disk with radius $R = (\pi/n)^{1/2}$. The negative heads concentrate around the counterion and make a negative disk with radius $R_- < R$ and charge density $-\sigma_-$ where $\sigma_- = \sigma/n\pi R_-^2 \geq \sigma$. The rest of the cell is occupied by neutral heads (Fig. 5). The fraction of negative heads $f^2 = R_-^2/R^2$ is fixed for each membrane. The uniform charge case is recovered when there are no neutral heads so that $R_- = R$ and $f = 1$.

Let us consider the weak screening case $r_s \gg R$. Under the transformation mentioned above, we add a disk with radius R , density $-\sigma^*$ to the Wigner-Seitz cell to neutralize it. Now, the total energy of a Wigner-Seitz cell is the sum of the interactions of the Z -ion with two disks of radiuses R_- and R , the self energy of the two disks and the interaction between the disks:

$$\begin{aligned} \varepsilon(n) = & -\frac{2\pi Ze\sigma_- R_-}{D} - \frac{2\pi Ze\sigma^* R}{D} + \frac{8\pi(\sigma_-)^2 R_-^3}{3D} \\ & + \frac{8\pi(\sigma^*)^2 R^3}{3D} + \int_{(R_-)} \int_{(R)} dr dr' \frac{\sigma_- \sigma^*}{D|\mathbf{r} - \mathbf{r}'|}. \end{aligned} \quad (84)$$

The integrations in the last term are taken over the disks with radius R_- and R respectively. This last term can be written as

$$\int_{(R_-)} \int_{(R)} dr dr' \frac{\sigma_- \sigma^*}{D|\mathbf{r} - \mathbf{r}'|} = \frac{2\pi\sigma_- \sigma^* R_-^3}{D} \mathcal{G}(f), \quad (85)$$

where $\mathcal{G}(f)$ is a function of f only and can be evaluated numerically for each value of f (it decreases monotonically from $8/3$ at $f = 1$ to 0 at $f = 0$). Using $Zen = \sigma + \sigma^*$ and Eq. (85), one gets from Eq. (84):

$$\begin{aligned} \varepsilon(n) = & -\frac{(Ze)^2}{RD} \left(2 - \frac{8}{3\pi}\right) + \frac{2\pi\sigma^2 R^3}{D} \left(\frac{4}{3f} + \frac{4}{3} - f\mathcal{G}(f)\right) \\ & + \frac{2\pi\sigma ZeR}{D} \left(1 - \frac{8}{3\pi} - \frac{1}{f} + \frac{f\mathcal{G}(f)}{\pi}\right). \end{aligned} \quad (86)$$

The last two terms is the correction to $\varepsilon(n)$ due to the mobility of the surface charge. In the uniform limit, $f = 1$, $\mathcal{G}(f) = 8/3$, these two terms vanish and one gets back the usual formula for the energy per ion of WC in Wigner-Seitz cell approximation, Eq. (15).

The chemical potential for a counterion in the mobile charge case, $\mu_{WC,m}$, can be easily calculated as

$$\mu_{WC,m} = \frac{\partial[n\varepsilon(n)]}{\partial n} \simeq -\frac{(Ze)^2}{RD} \left(2 + \frac{1}{f} + \frac{4}{3\pi f} - \frac{2f\mathcal{G}(f)}{\pi}\right). \quad (87)$$

Here σ is approximated by Zen , because at $r_s \gg R$, the ratio $\sigma^*/\sigma \ll 1$.

The ratio between chemical potential $\mu_{WC,m}$ for the mobile charges and the chemical potential μ_{WC} for the immobile charges has been evaluated numerically as function of the fraction f^2 of the negative heads. The result is plotted in Fig. 9.

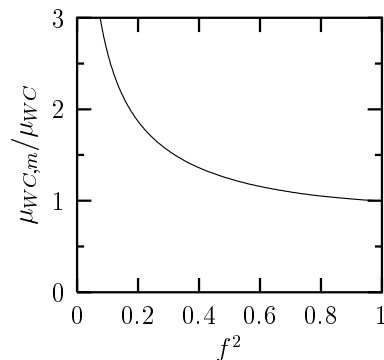


FIG. 9. The ratio between the chemical potentials $\mu_{WC,m}$ for the mobile charge case and μ_{WC} for the immobile charge case as a function of the fraction of charged heads f^2 .

Obviously, as f decreases, $\mu_{WC,m}$ grows as expected. According to Eq. (14) this means that the inversion ratio σ^*/σ grows with decreasing f , too. We do not continue the plot in Fig. 9 to very small f^2 because in this case, the entropy of negative heads plays important role and screening by negative heads of the membrane can be described in Debye-Hückel approximation²⁶. We do not consider this regime here.

Let us now move to the limit of strong screening, $r_s \ll R$. In this limit, it is more convenient to directly minimize the free energy, instead of using the capacitor model. Since $r_s \ll R$, one needs to keep only the nearest neighbour interactions in the free energy. Assuming $r_s \ll R_-$, one can write the free energy per unit area as

$$F = -2\pi\sigma_-r_sZen + 3n \left(Ze - \frac{\sigma}{n} \right)^2 \frac{\exp(-A/r_s)}{A}, \quad (88)$$

where $Ze - \sigma/n = \sigma^*/n$ is the charge of one Wigner-Seitz cell. In Eq. (88), the first term is the interaction of Z -ion with the negative background (the disk with charge density σ_-), the second term is the interaction between neighbouring Wigner-Seitz cells. As usual, the quadrupole-quadrupole interaction between Wigner-Seitz cells is neglected.

Minimizing the free energy (88) with respect to n , one gets $A \simeq r_s \ln(f^2\zeta)$ and

$$\frac{\sigma^*}{\sigma} = \frac{2\pi\zeta}{\sqrt{3}\ln^2(f^2\zeta)}, \quad (\zeta \gg 1). \quad (89)$$

where $\zeta = Ze/\pi\sigma r_s^2$. Comparing to Eq. (24), one can see that, as in the weak screening case, the inversion ratio increases due to the mobility of the surface charge.

Theory of this section is based on the assumption that the charge of Z -ion is so large that it is screened nonlinearly by the disk of opposite charge. One can easily generalize this calculations to rod-like polyelectrolytes and study the role of a similar stripe of positive hydrophilic heads attracted by strongly negative DNA. Note that the idea of nonlinear concentration of charge in membranes with two types of heads has been used recently in a theory of DNA-cationic lipid complexes²⁷.

IX. CONCLUSION

We would like to conclude with another general physical interpretation of the origin of charge inversion. To do so, let us begin with brief discussion of a separate physical problem, namely, let us imagine that, instead of a macroion, a neutral macroscopic metallic particle is suspended in water with Z - and mono-valent ions. In this case, each ion creates an image charge of opposite sign inside the metal and thus attracts to the metal. Obviously, this effect is by a factor Z^2 stronger for Z -ions than for monovalent ones. While directly at the

metal surface, energy of interaction of Z -ion with image, $-(Ze)^2/4a$, is much larger than $k_B T$. Therefore Z -ions are strongly bound to the metallic surface, making it effectively charged, while monovalent ions are loosely correlated with the surface, providing for its screening over the distances of the order of r_s . We can determine the net charge of metallic particle with bound Z -ions using the "capacitor model" discussed above. Namely, the attraction of the Z -ions to their images plays the role of correlation part of the chemical potential μ_c and provides for the voltage $Ze/4a$ which charges a "capacitor" with the width r_s between metal surface and the bulk solution. This leads to the result that metal surface is charged with the net charge density $\sigma^* = Zen = Ze/(16\pi ar_s)$. Note that metallic particle becomes charged due to interactions, or correlations, between Z -ions and their images, even though the particle itself was neutral in the first place.

Major results of the present paper can be now interpreted using a similar language of images^{2,3}. Although now we consider a macroion with an insulating body, it has some bare charge σ on its surface, which leads to adsorption of certain amount of Z -ions. The layer of adsorbed Z -ions plays the role of a metal. Indeed, consider bringing a new Z -ion to the macroion surface which has already some bound Z -ions. New Z -ion repels nearest adsorbed ones, creating a correlation hole for himself. In other words, it creates an image with the opposite charge behind the surface. Image attracts the Z -ion, thus providing for the negative μ_c in Eq. (11) and therefore leading to the charge inversion.

The analogy between the adsorbed layer of Z -ions and a metal surface holds only at length scales larger than some characteristic length. In WC this latter scale is equal to Wigner-Seitz cell radius R . This is why for WC $\mu_c \sim -(Ze)^2/R$ (see Eq. (17)). To make $|\mu_c| \gg k_B T$, small enough radius R is needed. This explains why a significant bare charge σ is necessary to initiate adsorption of Z -ions and to create a metallic layer with images which can lead to charge inversion. From formal point of view, charge inversion in this case can be characterized by the ratio σ^*/σ , as we did throughout the paper, while for a neutral metallic particle such ratio is infinite.

In this paper, we considered adsorption of rigid Z -ions with the shapes of either small spheres or thin rods. The concept of effective metallic surface and image based language is perfectly applicable in both cases. It appears also applicable to the other problem, not considered in this paper, namely, that of adsorption of a flexible polyelectrolyte on an oppositely charged dielectric macroion surface²⁸. To our mind, this idea was already implicitly used in Ref. 5, which assumes that Coulomb self-energy of a polyelectrolyte molecule in the adsorbed layer is negligible. This means that charge of the polyelectrolyte molecule is compensated by the correlation hole, or image. It is the image charge that attracts a flexible polyelectrolyte molecule to the surface. Interestingly, conformations of both the polymer molecule and its image

change when the molecule approaches the surface.

A similar role of images and correlations is actually well known in the physics of metals. In the Thomas-Fermi approximation (which is similar to PB one) the work function of a metal is zero²⁹ (the work function is an analog of μ_c). The finite value of the work function is known to result from the exchange and correlation between electrons. For a leaving electron it can be interpreted as interaction with its image charge in the metal²⁹.

We believe that interaction with image or, in other words, lateral correlations of Z -ions in the adsorbed layer is the only possible reason for a charge inversion exceeding one Z -ion charge (of course, we mean here purely Coulomb systems and do not speak about cases when charge inversion is driven by other forces, such as, e.g., hydrophobicity). In the Poisson-Boltzmann approximation, when charge is smeared uniformly along the surface, no charging of neutral metal or overcharging of charged insulating plane is possible.

ACKNOWLEDGMENTS

We are grateful to R. Podgornik and I. Rouzina for useful discussions. This work was supported by NSF DMR-9985985.

-
- ¹ J. Ennis, S. Marcelja and R. Kjellander, *Electrochim. Acta*, **41**, 2115 (1996)
² V. I. Perel and B. I. Shklovskii, *Physica A* **274**, 446 (1999).
³ B. I. Shklovskii, *Phys. Rev. E* **60**, 5802 (1999).
⁴ E. M. Mateescu, C. Jeppesen and P. Pincus, *Europhys. Lett.* **46**, 454 (1999); S. Y. Park, R. F. Bruinsma, and W. M. Gelbart, *Europhys. Lett.* **46**, 493 (1999);
⁵ J. F. Joanny, *Europhys. J. Phys. B* **9** 117 (1999); P. Sens, E. Gurovitch, *Phys. Rev. Lett.* **82**, 339 (1999).

- ⁶ R. R. Netz, J. F. Joanny, *Macromolecules*, **32**, 9013 (1999).
⁷ R. R. Netz, J. F. Joanny, *Macromolecules*, **32**, 9026 (1999).
⁸ Y. Wang, K. Kimura, Q. Huang, P. L. Dubin, W. Jaeger, *Macromolecules*, **32** (21), 7128 (1999).
⁹ T. Wallin, P. Linse, *J. Phys. Chem.* **100**, 17873 (1996); **101**, 5506 (1997).
¹⁰ P. L. Felgner, *Sci. American*, **276**, (6) 102 (1997).
¹¹ R. Messina, C. Holm, K. Kramer, Private communication.
¹² T. T. Nguyen, A. Yu. Grosberg, B. I. Shklovskii, *cond-mat/9912462*.
¹³ R. J. Hunter, *Foundations of colloid science*, Vol. 1, Oxford University Press (1986).
¹⁴ M. Gueron, G. Weisbuch, *Biopolymers*, **19**, 353 (1980); S. Alexander, P. M. Chaikin, P. Grant, G. J. Morales, P. Pincus, and D. Hone, *J. Chem. Phys.* **80**, 5776 (1984); S. A. Safran, P. A. Pincus, M. E. Cates, F. C. MacKintosh, *J. Phys. (France)* **51**, 503 (1990).
¹⁵ Ye Fang, Jie Yang, *J. Phys. Chem. B* **101**, 441 (1997).
¹⁶ R. J. Mashl, N. Grønbech-Jensen, M. R. Fitzsimmons, M. Lütt, DeQuan Li, *J. Chem. Phys. B* **110**, 2219 (1999).
¹⁷ G. S. Manning, *J. Chem. Phys.* **51**, 924 (1969).
¹⁸ L. Bonsall, A. A. Maradudin, *Phys. Rev.* **B15**, 1959 (1977).
¹⁹ R. C. Gann, S. Chakravarty, and G. V. Chester, *Phys. Rev. B* **20**, 326 (1979).
²⁰ H. Totsuji, *Phys. Rev. A* **17**, 399 (1978).
²¹ A. Yu. Grosberg, A. R. Khokhlov, *Statistical Physics of macromolecules*, AIP Press, New York (1994).
²² H. S. Harned, B. B. Owen, *Physical chemistry of electrolytic solutions*, Reinhold, New York (1963).
²³ M. Fixman, *J. Chem. Phys.* **70**, 4995 (1979).
²⁴ M. Gueron, J.-Ph. Demaret, *J. Chem. Phys.* **96**, 7816 (1992).
²⁵ For a charged plane charge inversion vanishes when $r_s \rightarrow \infty$. This conclusion, however can not be applied to a finite size macroion for which excessive charge saturates at the value $0.84\sqrt{QZe}$ when r_s exceeds the size of the macroion³.
²⁶ R. Menes, N. Grønbech-Jensen, P. Pincus, *cond-mat/9910223*
²⁷ R. Bruinsma, *Eur. Phys. J. B* **4**, 75 (1998).
²⁸ M. Rubinstein, Private communication.
²⁹ N. D. Lang, *Solid state physics*, Vol. 28, Edited by H. Ehrenreich, F. Seitz, and D. Turnbull, Academic Press, New York, 1973